Journal of Power Sources 192 (2009) 408–413

Contents lists available at ScienceDirect

Journal of Power Sources

journal homepage: www.elsevier.com/locate/jpowsour

Investigation on silver electric adhesive doped with Al_2O_3 ceramic particles for sealing planar solid oxide fuel cell

Xiaoliang Zhou [a,b,c], Kening Sun [a,c,*], Yan Yan [c], Shiru Le [a,c], Naiqing Zhang [a,c], Wang Sun [c], Peng Wang [b]

[a] Science Research Center, Academy of Fundamental and Interdisciplinary Sciences, Harbin Institute of Technology, Harbin 150080, PR China
[b] School of Municipal and Environmental Engineering, Harbin Institute of Technology, Harbin 150090, PR China
[c] Department of Applied Chemistry, Harbin Institute of Technology, No. 92 of West Dazhi Street, P.O. Box 211, Harbin 150001, PR China

ARTICLE INFO

Article history:
Received 26 February 2009
Received in revised form 24 March 2009
Accepted 24 March 2009
Available online 2 April 2009

Keywords:
Solid oxide fuel cell
Sealing
Silver electric adhesive
Alumina ceramic particles

ABSTRACT

The silver electric adhesive doped with Al_2O_3 ceramic particles is used as sealing material for planar solid oxide fuel cell (SOFC). The sealing temperature of this sealing material is 600 °C with the heating rate of 2 °C min^{-1}, and the minimal leak rate ranges from 0.030 sccm cm^{-1} to 0.040 sccm cm^{-1}. When doping 15 mass% Al_2O_3 ceramic particles into this sealing material, the thermal expansion coefficient of this material decreases from 20 ppm K^{-1} to 15 ppm K^{-1}, which improves the thermal matching performance and the long-term stability of the material significantly. When using the gradient sealing method with the pure silver electric adhesive and the silver electric adhesive doped with Al_2O_3 ceramic particles to seal the interface of Ni-YSZ/SUS430 in the simulating cell, the minimal leak rate of 0.035 sccm cm^{-1} is obtained for the cell. Furthermore, the simulating cell sealed with the compound silver electric adhesive presents good heat-resistant impact ability. Therefore, this compound sealing technique is a very promising sealing method for SOFC.

1. Introduction

Planar intermediate temperature solid oxide fuel cells (IT-SOFCs) have attracted intensive attention since the end of last century by virtue of reduced operation temperature, high power density, simple configuration, easy assembly, metallic interconnects and low cost manufacturing [1]. Among the technical challenges in developing planar SOFCs, the sealing material has been regarded as one of the most significant issues [2,3]. So far, many seal types have been explored, including rigid glass or glass-ceramic materials [4–6], deformable metallic materials [7,8], braze-based rigid seals [9,10], and metal or mica-based seals [11–16]. The advantage of glass based seals is that their compositions can be tailored to optimize the required physical properties, such as the coefficient of thermal expansion (CTE); nevertheless, they tend to change in phases and react with the cell component materials and interconnects under SOFC operating conditions in a long run, because of the intrinsic thermo-dynamical instability [17,18]. The plain mica is virtually incompressible; a considerable compressive stress is required to obtain satisfied sealing effect, which may cause cell breakages. The hybrid mica-based seals [11–15] have achieved quite low leakage rate, but the sealing processes become more complex and other issues, such as stability and compatibility, have remained unsolved. The application of the deformable metallic seals is limited by its high electronic conductivity.

The requirements for a metal sealing material that joins ceramic and metal parts in an SOFC are that it (i) bonds to the joining members, (ii) provides a crack-free joint after brazing and during use, (iii) provides a joint with no interconnected porosity, (iv) is stable when simultaneously exposed to fuel and oxidizing atmosphere, (v) does not contain entities that could contaminate other materials of the fuel cell and, in the case that the metal sealing material is a part of the current path, (vi) has a high electrical conductivity [4]. The metal material must seal at the electrolyte and interconnect surfaces and provide electrical connection and a strong bond between the yttria-stabilized zirconia (YSZ) and metal interconnect. However, the CTE of most metal materials is in the range 16–21 ppm K^{-1}, for instance Ag-based alloys are at the higher end of this range. The CTE of YSZ is 10.5 ppm K^{-1}. This CTE mismatch is sufficient to cause cracking in an YSZ joining member after brazing. Even if a crack-free joint can be produced, the thermal cycling of the joint during operation will produce cracks at the braze/YSZ interface [19]. Such cracking is clearly detrimental to the gas-sealing, strength and lifetime of the joint, and is therefore unacceptable.

There are many strategies to minimize the thermal stress in a metal joint. For instance, the metal joint can include a metal foil or mesh that either has a low CTE, thus reducing the bulk CTE of

* Corresponding author at: Science Research Center, Academy of Fundamental and Interdisciplinary Sciences, Harbin Institute of Technology, Harbin 150080, PR China. Tel.: +86 451 86412153; fax: +86 451 86412153.
E-mail address: keningsun@yahoo.com.cn (K. Sun).

0378-7753/$ – see front matter © 2009 Elsevier B.V. All rights reserved.
doi:10.1016/j.jpowsour.2009.03.047

the joint, or has a low Young's modulus so as to accommodate mechanical strain. The addition of cladding metals or foil members to the joint may, however, have undesirable consequences for thickness, lifetime, oxidation stability, chemical stability, etc., of the joint. Another strategy is to fill the metal joint with particles that have a lower CTE than the metal sealing material, resulting in a composite metal material with a bulk CTE that is more closely matched to that of the joining members. Ishikawa et al. [20] disclosed a joint wherein the gap between two fitted bonding members was filled with a hard solder and particulate filler, resulting in a composite joint material after soldering. The volume fraction of the particulate filler is specified to be 30–90% of the total composite filler. Shinkai and Kida [21] disclosed a bonding system in which a hard solder is filled with at least two types of particulates differing in wettability with the solder.

In this paper, a modified silver electric adhesive material that is especially well-suited for sealing and interconnecting anode-supported SOFCs was introduced. The coefficient of thermal expansion of a commercial silver electric adhesive was adjusted by filling with ceramic particles. Thermal cycling ability, thermal stability, and possible application in joining YSZ to stainless steel of SOFC interconnects were evaluated.

2. Experimental details

2.1. Materials

DAD-87 silver electric adhesive (Shanghai, China) was mainly composed of epoxy resin, silver and organic solvents. Solidified agents were the heat-resistant epoxy and phenolic resin, in which the molecules contain more benzene ring structures so that a high cross-linking density could be obtained after solidification. The main characteristics of DAD-87 silver electric adhesive are listed in Table 1. The average particle size of Al_2O_3 ceramic powder is 7.87 μm. The substrate of the cell was Ni-YSZ/YSZ (8 mol% Y_2O_3 stabilized ZrO_2) fabricated by tape casting with a diameter of 19 mm. LSM ($La_{0.7}Sr_{0.3}MnO_3$) cathode powders were screen printed onto the surface of the electrolyte. SUS430 (16% Cr, 1% Mn, 0.75% Si, bal. Fe) was used as the interconnect.

2.2. The sealing method and process

Due to the gelatinousness of the electric adhesive at room temperature, it can be coated onto the sealed components directly following by solidifying at 80 °C for 2 h in the oven, and then the organic additive can be burned down in the furnace by heating with a rate of 2 °C min^{-1} till the temperature reaches 600 °C and being held for 30 min at this temperature. Interconnect (SUS430) and PEN (Positive Electrolyte Negative) were assembled in a sequence of interconnect/sealing material/PEN.

2.3. Volatilization test of the silver electric adhesive

The silver electric adhesive was screen printed on a dense Al_2O_3 disc, and then the disc was heated up to 800 °C and held for 15 min at this temperature. After cooling down to room temperature, the weight of disc was measured. Subsequently, the disc was put into a quartz tube and reheated up to 800 °C and held for 52 h at this temperature. Air was used as the flowing gas with a flow rate of 150 sccm. The exposed area was 2 cm × 2 cm. After the exposure at high temperature, the weight was determined using the balance with the measurement precision of 0.0001 g.

Table 1
The main characteristics of DAD-87 silver electric adhesive*.

Viscosity (25 °C)	20 ± 5 Pa s
Ag content	≥82%
Ag particle size	1 μm
Volume electrical resistivity	(1–5) × 10^{-4} Ω cm
Shearing strength (25 °C)	≥4 MPa

* Data were provided by Shanghai Research Institute of Synthetic Resins, Shanghai, China.

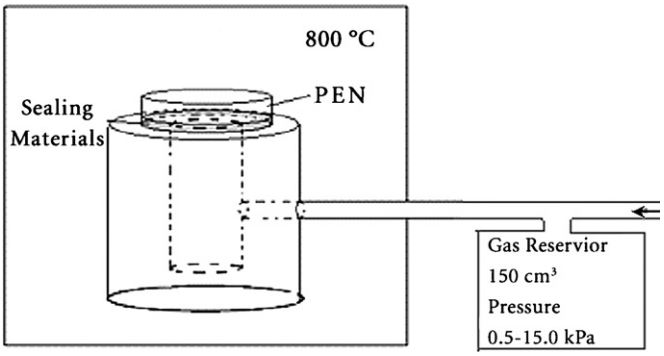

Fig. 1. Schematic of leak rate test for the simulating cell.

2.4. Leak rate test

A PEN cylinder and a SUS430 steel plate were sealed and then heated to 800 °C. A 150 cm^3 gas reservoir was kept under ambient conditions and connected to the samples via a 1 mm inner diameter SUS430 tube. Two pressures: 1.4 kPa and 15.0 kPa were used. 1.4 kPa is likely to be close to the actual planar SOFC pressure [22] while 15.0 kPa may be considered as an upper limit. The line between the nitrogen source and the reservoir was then closed, and the resulting pressure decayed in the reservoir with respect to time from 15.0 kPa to 2.0 kPa or 1.4 kPa to 0.5 kPa. A schematic of the leak rate test is illustrated in Fig. 1. From the pressure decay versus time data, leak rates could subsequently be calculated using the equation below [14,23]:

$$L = \frac{(P_i - P_f)V}{P_f \Delta t C}$$

where L is the leak rate, sccm cm^{-1} (standard-state cubic centimeter per minute per centimeter), V the reservoir volume and SUS430 steel column pipe and P is the gas pressure. Subscripts i and f represent the initial and final conditions and C is the outer length of the SUS430 cylinder circumference.

2.5. Thermal cycling test

Thermal cycling test of the samples in air environment was conducted to evaluate the stability of the sealant. The sealed samples were heated from room temperature to 800 °C at a heating rate of 10 °C min^{-1}, situated at 800 °C for 60 min for the leakage test and then cooled to 400 °C at a cooling rate of 10 °C min^{-1}, finally was freely cooled down to room temperature. The temperature profile for the thermal cycling is shown in Fig. 2. The total cycling times were 10.

2.6. Open circuit voltage test

The unit cell was prepared by co-firing a tri-layer substrate at 1400 °C for 4 h. The tri-layer substrate is composed of NiO-YSZ anode support, anode functional layer and YSZ electrolyte layer prepared by co-tape casting. A functionally graded cathode composed of LSM-YSZ and LSM layers was formed onto the electrolyte layer by screen printing and sintering at 1150 °C for 2 h. The sealant was printed between the anode face of the unit cell and metal inter-

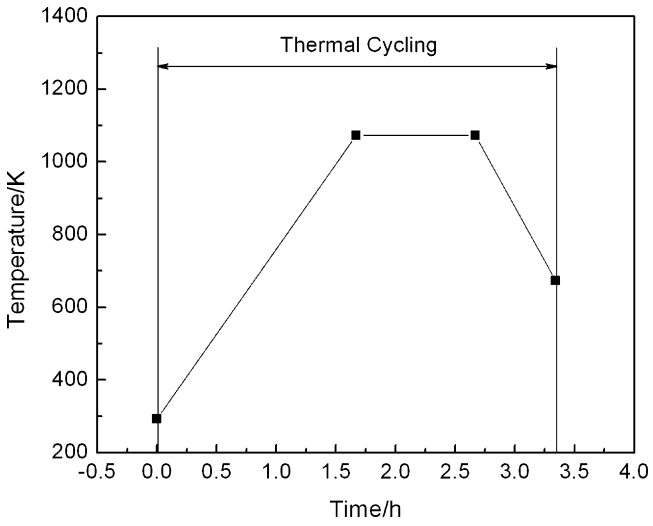

Fig. 2. Temperature profile for thermal cycling.

connect. After maintaining the unit cell at 800 °C for 30 min, OCV measurements were initiated. The holding time of the unit cell was 10 h. A hydrogen containing gas (H_2 + 3%H_2O) was used as a fuel at a flow rate of 50 sccm while the cathode was exposed to the stationary air.

The morphology of the samples with polished cross-sections was examined using a HITACHI S4700 scanning electron microscopy (SEM). The thermal expansion was measured at 30–850 °C using a dilatometer (DIL402PC, Germany) at a heating rate of 2 °C min^{-1}.

3. Results and discussion

3.1. Investigation on the volatilization of the silver electric adhesive at high temperature

The volatilization of silver due to its relatively low melting point, high volatility and rapid thermal etching in hot air [24,25], may limit its use in SOFCs operating at relatively high temperatures. Considering the relatively low melting point of the silver metal, we tested the volatilization rate of the silver electric adhesive at 800 °C. The changing of the mass of the silver electric adhesive during the holding time of 52 h is shown in Fig. 3, in which the symbols a, b and c stand for the samples of the silver electric adhesive with different initial mass, respectively. From Fig. 3, it can be seen that for all the samples, nearly no mass loss of the samples was observed after experiencing 52 h at 800 °C. This indicated that the volatilization rate of the silver electric adhesive at high temperature of 800 °C was very low and that this sealant could be applied for the long-term operation. Therefore, as far as the high temperature volatilization is concerned, the silver electric adhesive can be adopted for sealing the planar SOFC.

3.2. The use of silver electric adhesive in sealing simulating cell

After sealed with three coating layers of silver electric adhesive, the leak rate of the simulating cell was measured. The average leak rate was between 0.030 sccm cm^{-1} and 0.040 sccm cm^{-1}. In addition, in order to evaluate sealing performance and thermo-mechanical stability of the sealant, open circuit voltage (OCV) of the unit cell was measured. The relationship between OCV and the holding time is shown in Fig. 4. The decrease on hydrogen partial pressure is associated with the decrease on cell voltage, and it is consistent with the leak rate. The OCV of the simulating cell was 1.10 V which is close to theoretical OCV of 1.19 V. After six hours maintenance, the OCV was above 1.05 V and did not decrease any more, indicating the leak rate gained the stability after a period of time. And there was almost no remarkable change in OCV occurred after the holding time of 10 h, indicating gas tightness of the simulating cell sealed with the silver electric adhesive is favorable for meeting the requirements of SOFC working conditions.

However, when the silver electric adhesive was used to seal the single cell whose dimension is larger than the simulating cell, the leak rate increased rapidly, especially after thermal cycling. This is probably due to the visible cracks in the single cell wall which were caused by CTE mismatch between the silver electric adhesive and the single cell wall.

3.3. Matching CTE of the silver electric adhesive to the components of SOFC

Fig. 5 shows the CTE curves of the silver electric adhesive and the components of SOFC. The CTEs were determined from the slope of the strain versus temperature plots. The CTE of interconnect was between 10 ppm K^{-1} and 12 ppm K^{-1}, and that of YSZ was about 9 ppm K^{-1}, the CTE of Ni-YSZ was higher than that of YSZ, about 10 ppm K^{-1}. This indicated that interconnect was matching with

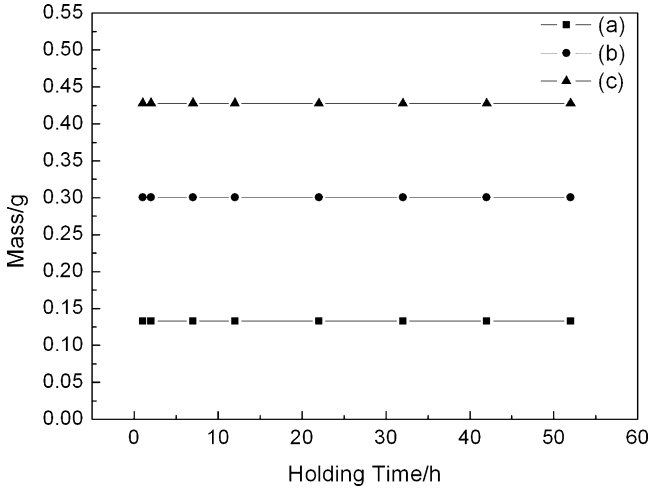

Fig. 3. The dependence of the silver electric adhesive with different initial mass on the holding time at 800 °C: (a) 0.1331 g, (b) 0.3004 g, (c) 0.4280 g.

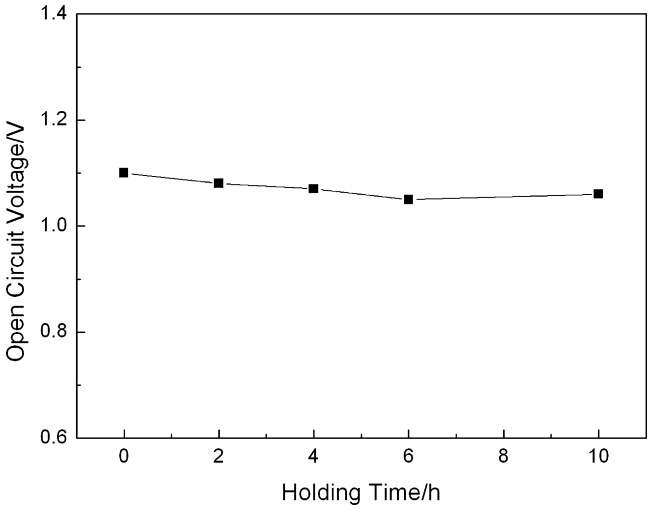

Fig. 4. Change of open circuit voltage with the holding time.

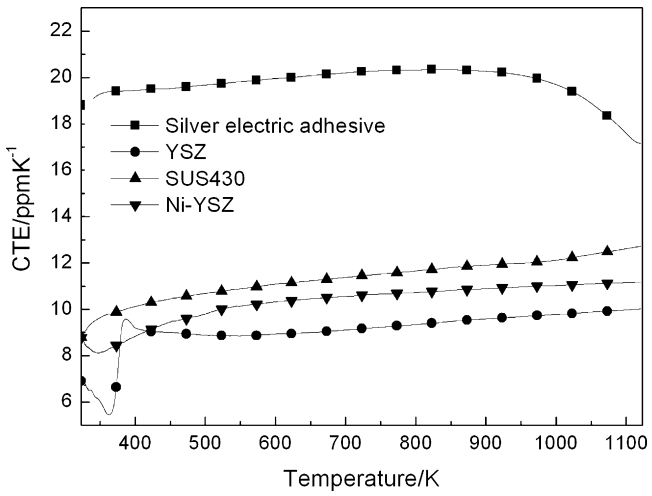

Fig. 5. Thermal expansion curves of silver electric adhesive and the SOFC components.

YSZ and Ni-YSZ. The CTE of silver electric adhesive was 20 ppm K^{-1} at low temperature range and it started dropping from 923 K as shown in Fig. 5.

According to the above results obtained, Al_2O_3 ceramic particles were chosen to be doped into the silver electric adhesive in order to change the coefficient of thermal expansion. The amount of the Al_2O_3 particles, 5 mass%, 10 mass%, 15 mass% and 20 mass%, was investigated. When the amount of the dopant Al_2O_3 was 20 mass%, it was found that the silver electric adhesive showed unfavorable cohesive ability, and could not be fabricated to be the sample that met the request of the coefficient of thermal expansion test. The change of the coefficient of thermal expansion of the silver electric adhesive with different amount of the dopant Al_2O_3 is demonstrated in Fig. 6. It was found that the coefficient of thermal expansion reduced obviously with the increase of the dopant Al_2O_3. Furthermore, the decreasing trend at the high temperature was decrescent. This means that dopant Al_2O_3 ceramic particles could obviously improve the thermal match between the silver electric adhesive and the components of the fuel cell.

The influence of Al_2O_3 doping amount on the leak rate is shown in Table 2. From Table 2, it can be seen that the leak rates of the simulating cells increased after Al_2O_3 ceramic particles were doped into the silver electric adhesive. When the doping content was increased

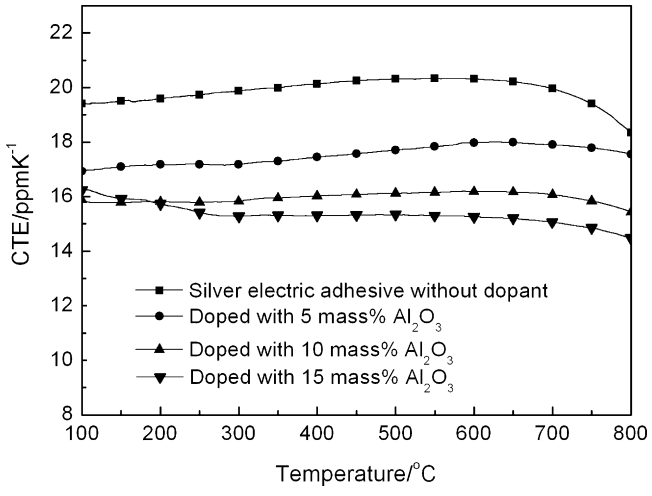

Fig. 6. Thermal expansion of silver electric adhesive with different doping amounts.

Table 2
Influence of Al_2O_3 doping amount on leak rates of the simulating cells.

Al_2O_3 content (mass%)	Leak rate (sccm cm^{-1})
5	2.8
10	6.4
15	6.1
20	16

to 20 mass%, the leak rate of the simulating cells increased substantially, and the bond strength of those was found very low.

The SEM micrographs of the SUS430/electric adhesive with dopant Al_2O_3/Ni-YSZ sealing interface are shown in Fig. 7. The amount of the dopant Al_2O_3 was 5 mass%, 10 mass%, 15 mass% and 20 mass%, respectively. In the Fig. 7(a), cracks were found at the interface of the Ni-YSZ/silver electric adhesive and the interface of the silver electric adhesive/SUS430 when the amount of the dopant Al_2O_3 was 20 mass%, and some holes were also found inside the silver electric adhesive. These results basically matched the rapidly rising leakage of the simulating cell which was sealed with the silver electric adhesive doped with 20 mass% Al_2O_3 as shown in Table 2.

Fig. 7(b) shows the sealing interface of the electric adhesive doped with the 15 mass% Al_2O_3. From this micrograph, it can be seen that Ni-YSZ, silver electric adhesive and SUS430 integrated tightly. However, there were still some holes inside the silver electric adhesive. Fig. 7(c) and (d) shows the sealing interface of the silver electric adhesive doped with 10 mass% and 5 mass% Al_2O_3 respectively. It can be seen that these two micrographs are similar. The Ni-YSZ, silver electric adhesive and SUS430 integrated tightly, and the Al_2O_3 ceramic particles in the silver electric adhesive showed uniform distribution. Although some micro-holes were still found inside the silver electric adhesive, the quantity was evidently less than the silver electric adhesive doped with 15 mass% and 20 mass% Al_2O_3 ceramic particles.

3.4. Sealing using the gradient compound sealing technique

In order to enhance the gas tightness of the silver electric adhesive doped with Al_2O_3, the sealing method was changed to the gradient compound sealing technique in which the pure silver electric adhesive and the silver electric adhesive doped with the Al_2O_3 ceramic particles were used as the gradient compound. The layer thickness was 40 μm for sealant with alumina and 10 μm for sealant without alumina. The leak rates of the simulating cells sealed by the gradient compound were tested, and the results are shown in Table 3.

As shown in Table 3, with the improved sealing technique, the first layer was coated with the silver electric adhesive doped with Al_2O_3, then other two layers with pure silver electric adhesive. The leak rate of the simulating cell was obviously decreased, ranging between 0.030 sccm cm^{-1} and 0.050 sccm cm^{-1}. When the silver electric adhesive doped with 15 mass% Al_2O_3 ceramic particles was used for the first layer, doped with 5 mass% Al_2O_3 for the second layer, and no dopant for another two layers, the leak rate of the simulating cell achieved the minimal value, about 0.035 sccm cm^{-1}.

Table 3
Influence of gradient compound sealing on leak rates of the simulating cells.

Al_2O_3 content in gradient compound (mass%)				Leak rate (sccm cm^{-1})
1st layer	2nd layer	3rd layer	4th layer	
5	0	0	–	0.039
10	0	0	–	0.045
15	0	0	–	0.046
15	5	0	0	0.035

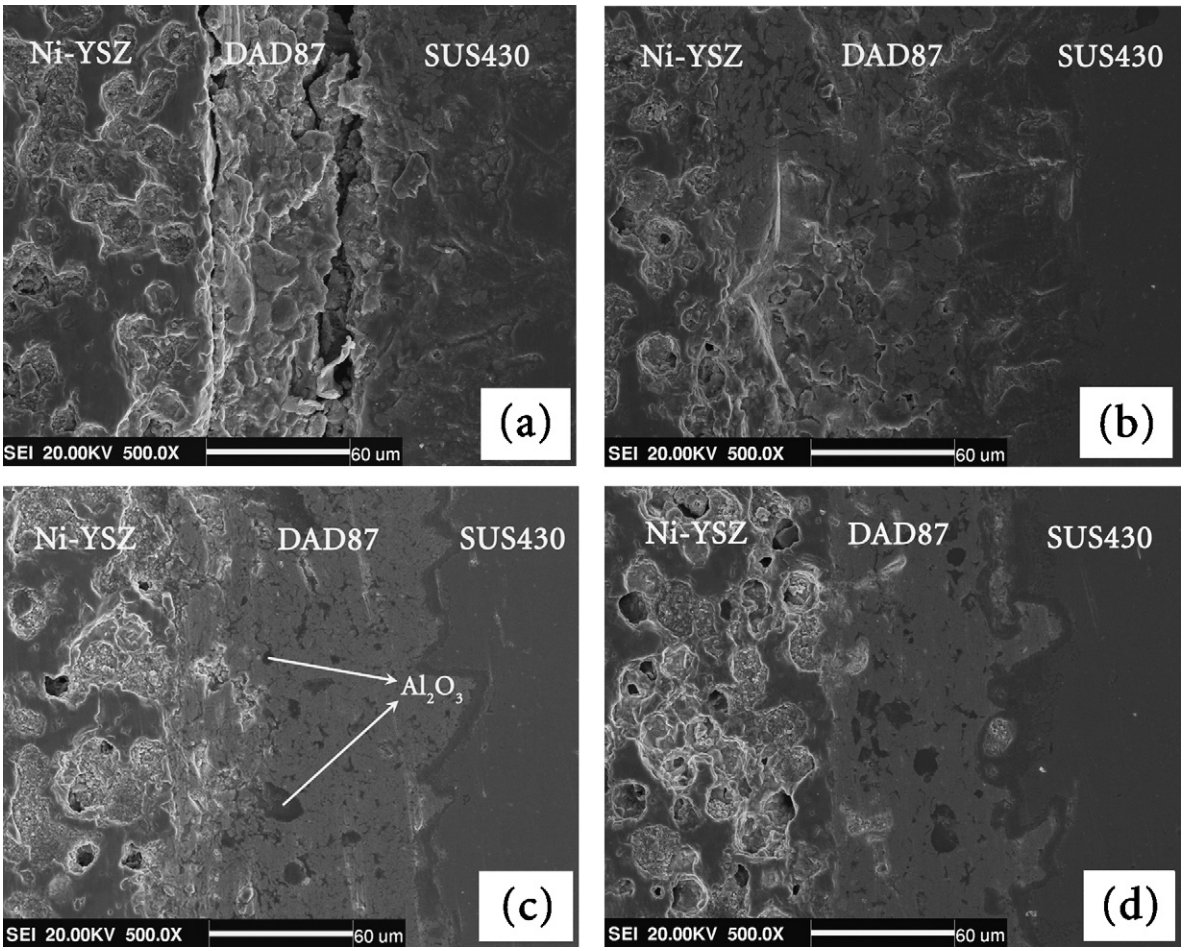

Fig. 7. SEM micrographs of the SUS430/Electric adhesive with dopant Al_2O_3/Ni-YSZ sealing interface: (a) 20 mass% Al_2O_3, (b) 15 mass% Al_2O_3, (c) 10 mass% Al_2O_3, (d) 5 mass% Al_2O_3.

The leak rates for the layered seals are about the same as those for the seals without alumina. The advantage of the alumina additions is to improve the thermal cycling conditions. The seals without alumina were tested under thermal cycling conditions. The results indicated the leak rate decreased very fast after experiencing several thermal cycling, which was contributed to the mismatch of the binder and electrolyte/SUS430.

3.5. *Effects of thermal cycling on the leak rate of the simulating cells*

In order to test the heat-resistant impact ability of the simulating cells which were sealed with the silver electric adhesive, the leak rate of the simulating cells was measured after 10 thermal cycles with the first sealing layer of silver electric adhesive with 15 mass% Al_2O_3, the second sealing layer doped with 5 mass% Al_2O_3 and the outer two sealing layers of pure silver electric adhesive. The multilayer sealing approach can improve the thermo-mechanical stability of the sealant and thermal cycling stability, which was contributed to the improvement of the CTEs compatibility. Moreover, using this sealing method, the lower leak rate can be obtained due to the good sealing performance of the silver electric adhesive. As shown in Fig. 8, the leak rate of the simulating cell was stable during all of the 10 thermal cycles, indicating that the simulating cell sealed with the gradient compound had good heat-resistant impact ability.

Fig. 9 shows the SEM micrograph of the sealing interface of Ni-YSZ/electric adhesive and the electric adhesive with alumina/SUS430 after 10 thermal cycles. As shown in the micrograph, the sealing interface was still integrated tightly after experiencing 10 thermal cycles. No significant change was found at the interface. It turned out that the thermal cycling resistance of the silver electric adhesive was good. As a result, this gradient compound sealing technique is a very promising sealing method for the practical application of SOFC.

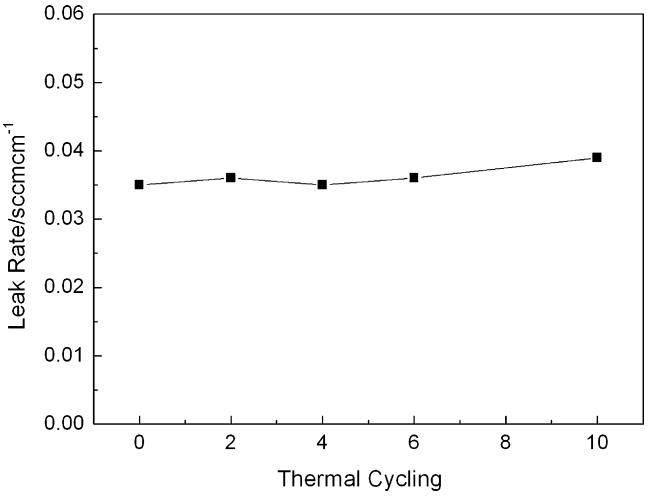

Fig. 8. Leak rate change of the simulating cell during 10 thermal cycles.

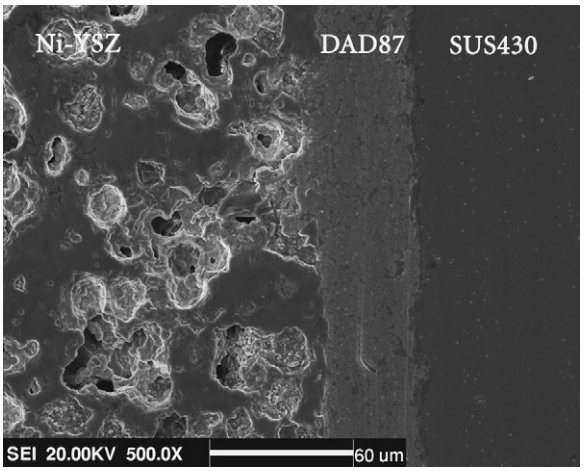

Fig. 9. SEM micrograph of the sealing interface after 10 thermal cycles.

4. Conclusions

The silver electric adhesive doped with Al_2O_3 ceramic particles was used as the sealing material for planar SOFC. The leak rates of the simulating cells sealed with the silver electric adhesive were between 0.030 sccm cm^{-1} and 0.040 sccm cm^{-1}. The open voltage was stable at 1.05 V within 10 h. In order to match the thermal expansion of the silver electric adhesive with that of the components of the cell, Al_2O_3 ceramic particles were doped into the silver electric adhesive. The thermal expansion coefficient of the silver electric adhesive was decreased from 20 ppm K^{-1} to 15 ppm K^{-1}. Aiming at enhancing the gas tightness of the silver electric adhesive doped with Al_2O_3, the gradient compound sealing technique was adopted, and the minimal leak rate 0.035 sccm cm^{-1} was obtained. After 10 thermal cycles, the leak rate of the simulating cell was still in the range of 0.035–0.040 sccm cm^{-1}, which indicates that the simulating cell had fine heat-resistant impact ability. Therefore, the silver electric adhesive doped with Al_2O_3 ceramic particles and the gradient compound sealing technique will be very promising for sealing planar SOFC.

Acknowledgements

This project is financially supported by Development Program for Outstanding Young Teachers in Harbin Institute of Technology (no. HITQNJS.2008.056), China Postdoctoral Science Foundation (no. 20070420865), and Natural Science Foundation of China (no. 90510006).

References

[1] S.C. Singhal, J. Mizusaki (Eds.), Solid oxide fuel cells-IX, the Electrochemical Society Proceedings, Pennington, NJ, 2005.
[2] G.J. La O', H.J. In, E. Crumlin, G. Barbastathis, Y. Shao-Horn, Int. J. Energ. Res. 31 (2007) 548–575.
[3] H.W. Lee, S.M. Kim, H. Kim, H.Y. Jung, H.G. Jung, J.H. Lee, H. Song, H.R. Kim, J.W. Son, Solid State Ionics 179 (2008) 1454–1458.
[4] W.F. Jeffrey, J. Power Sources 147 (2005) 46–57.
[5] Z.G. Yang, G.G. Xia, K.D. Meinhardt, J. Mater. Eng. Perform. 13 (3) (2004) 327–335.
[6] F. Smeacetto, M. Salvo, M. Ferraris, J. Cho, A.R. Boccaccini, J. Eur. Ceram. Soc. 28 (1) (2008) 61–68.
[7] K.S. Weil, J.S. Hardy, Ceram. Eng. Sci. Proc. 25 (3) (2004) 321–326.
[8] J. Duquette, A. Petric, J. Power Sources 137 (1) (2004) 71–75.
[9] A. Atkinson, B. Sun, Mater. Sci. Technol. 23 (10) (2007) 1135–1143.
[10] M.C. Tucker, C.P. Jacobson, L.C. De Jonghe, S.J. Visco, J. Power Sources 160 (2006) 1049–1057.
[11] Y.S. Chou, J.W. Stevenson, J. Power Sources 135 (1–2) (2004) 72–78.
[12] S.P. Simner, J.W. Stevenson, J. Power Sources 102 (1–2) (2001) 310–316.
[13] Y.S. Chou, J.W. Stevenson, J. Power Sources 124 (2) (2003) 473–478.
[14] Y.S. Chou, J.W. Stevenson, L.A. Chick, J. Power Sources 112 (1) (2002) 130–136.
[15] Y.S. Chou, J.W. Stevenson, L.A. Chick, J. Am. Ceram. Soc. 86 (6) (2003) 1003–1007.
[16] Y.S. Chou, J.W. Stevenson, P. Singh, Ceram. Eng. Sci. Proc. 26 (4) (2004) 257–264.
[17] S.P. Jiang, L. Christiansen, B. Hughan, K. Foger, J. Mater. Sci. Lett. 20 (8) (2001) 695–697.
[18] Z.G. Yang, J.W. Stevenson, K.D. Meinhardt, Solid State Ionics 160 (2003) 213–225.
[19] M. Singh, T.P. Shpargel, R. Asthana, Mater. Sci. Eng. A: Struct. Mater. Prop. Microstruct. Process. 485 (2008) 695–702.
[20] T. Ishikawa, M. Shinkai, M. Kida, US Patent 6,348,273 (2002).
[21] M. Shinkai, M. Kida, US Patent 6,565,621 (2003).
[22] W.X. Li, K. Hasinska, M. Seabaugh, S. Swartz, J. Lannutti, J. Power Sources 138 (1–2) (2004) 145–155.
[23] S.R. Le, K.N. Sun, N.Q. Zhang, Y.B. Shao, M.Z. An, Q. Fu, X.D. Zhu, J. Power Sources 168 (2007) 447–452.
[24] B. Chalmers, R. King, R. Shuttleworth, Proc. R. Soc. A193 (1948) 465.
[25] E.D. Hondros, A.J.W. Moore, Acta Metall. 8 (1960) 647.